INTERACTION OF LOW-ENERGY POSITRONS WITH ATOMS AND MOLECULES: SCATTERING, BOUND STATES, PS FORMATION AND ANNIHILATION

GLEB GRIBAKIN

Department of Applied Mathematics and Theoretical Physics
Queen's University, Belfast BT7 1NN, Northern Ireland
E-mail: g.gribakin@am.qub.ac.uk

This paper reviews the progress in our understanding of positron interaction with atoms and molecules made over the past few years. The analysis is based on atomic many-body theory which allows one to identify different contributions to the positron-atom interaction. In particular, the role of virtual positronium formation which increases the attraction between the positron and atomic system is highlighted. Its contribution is additional to the the usual polarisation potential which behaves as $-\alpha e^2/2r^4$ at large distances and which affects both electron- and positron-atom scattering. For heavier noble gas atoms this leads to positron virtual s levels which enhance elastic scattering and positron-atom annihilation at low energies. For species with larger dipole polarisabilities α and somewhat smaller ionisation potentials, e.g. Mg, the strong attraction results in positron-atom *bound* states. It turns out that such bound states can provide an explanation for huge and chemically sensitive positron annihilation rates observed for polyatomic molecules, in terms of positron-molecule vibrational Feshbach resonances.

1 Many-Body Theory Approach to the Positron-Atom Interaction

Many-body theory allows one to describe the interaction of a positron (or an electron) with a many-electron atom in terms of a single-particle equation (see, e.g. [1,2])

$$H_0\psi_\varepsilon(\mathbf{r}) + \int \Sigma_\varepsilon(\mathbf{r},\mathbf{r}')\psi_\varepsilon d\mathbf{r}' = \varepsilon\psi_\varepsilon(\mathbf{r}), \tag{1}$$

where ψ_ε is the so-called quasi-particle wavefunction with the energy ε relative to the ground-state energy of the target, H_0 is the single-particle Hamiltonian, usually chosen to be the Hartree-Fock (HF) Hamiltonian of the target atom, and Σ_ε is a nonlocal energy-dependent correlation "potential". It accounts for the interaction between the extra particle[a] and the atom beyond the HF approximation.

The wavefunction $\psi_\varepsilon(\mathbf{r})$ is equal to the projection of the exact total $N+1$-particle wavefunction of the system onto the N-electron ground-state wavefunction of the target,

$$\psi_\varepsilon(\mathbf{r}) = \int \Psi_0^*(\mathbf{r}_1,\ldots,\mathbf{r}_N)\Psi_E(\mathbf{r}_1,\ldots,\mathbf{r}_N,\mathbf{r})d\mathbf{r}_1\ldots d\mathbf{r}_N, \tag{2}$$

where $E = E_0 + \varepsilon$, and E_0 is the target ground-state energy. Although $\psi_\varepsilon(\mathbf{r})$ is a much simpler quantity than $\Psi_E(\mathbf{r}_1,\ldots,\mathbf{r}_N,\mathbf{r})$, it still contains a lot of information about the system. For example, at energies E above E_0 but below the excitation threshold of the target, Ψ_E describes elastic scattering. At large positron-atom separations it has the following

[a] For the sake of definiteness in what follows we talk of the positron. Of course, the general approach applies to the electron-atom interaction as well. The only difference between the two cases is that for the electron, both H_0 and Σ_ε must include exchange.

asymptotic form

$$\Psi_E(\mathbf{r}_1,\ldots,\mathbf{r}_N,\mathbf{r}) \simeq \Psi_0(\mathbf{r}_1,\ldots,\mathbf{r}_N)\left(e^{i\mathbf{k}\cdot\mathbf{r}} + f_{\mathbf{k}\mathbf{k}'}\frac{e^{ikr}}{r}\right), \tag{3}$$

where $\mathbf{k}$ is the initial positron momentum, $\varepsilon = k^2/2$ (we use atomic units where $\hbar = m_e = |e| = 1$), and $f_{\mathbf{k}\mathbf{k}'}$ is the scattering amplitude, $\mathbf{k}'$ being the final-state momentum. It follows from Eq. (2) that $\psi(\mathbf{r})$ has the same asymptotic behaviour as the term in brackets. Hence, it "knows" everything about the scattering phaseshifts and allows one to calculate the scattering cross section.

If a positron-atom bound state exists at $E < E_0$, Eq. (1) has a negative eigenvalue $\varepsilon_0 = E - E_0$, and the corresponding wavefunction $\psi_0(\mathbf{r})$ has the correct asymptotic behaviour of a bound state, $\psi_0(\mathbf{r}) \simeq Ar^{-1}e^{-\kappa r}$, where κ is determined by the binding energy, $\kappa = \sqrt{-2\varepsilon_0}$ (and s-wave binding is assumed). To see that the quasi-particle many-body description is not just a single-particle approximation, consider the normalisation integral for $\psi_0(\mathbf{r})$. Using the Cauchy-Schwartz inequality together with the fact that Ψ_E and Ψ_0 are normalised to unity, we have $\int |\psi_0(\mathbf{r})|^2 d\mathbf{r} \leq 1$. This integral is the probability that in the positron-atom bound state the atom remains in the ground state while the positron occupies a particular single-particle orbital. Therefore, the formalism accounts for the atomic and positron excitations which reduce the normalisation integral compared to unity.

Equation (1) effectively describes the motion of the positron in the field of a many-electron target. The operator H_0 describes the interaction of the positron with the nucleus and the self-consistent mean field of the target electrons. Its eigenstates form a complete basis of single-particle states. It serves as a starting (zeroth-order) approximation for the description of the system. It can also be used to account for the interaction between the particles beyond the mean-field approximation (i.e. *correlations*) by means of many-body perturbation theory.

All the dynamics of the many-body problem is hidden in $\Sigma_\varepsilon(\mathbf{r},\mathbf{r}')$. In some sense, its calculation is equivalent to solving the full $N+1$-particle Schrödinger equation. From a formal point of view, Σ_ε is equal to the self-energy operator of the single-particle Green's function.[3] This allows one to present it as an infinite perturbation series in powers of the electron-positron and electron-electron interaction (see below).

For small projectile energies $|\varepsilon| \ll I$, where I is the ionisation potential of the atom, the correlation potential has a well-known long-range asymptotic behaviour

$$\Sigma_\varepsilon(\mathbf{r},\mathbf{r}') \simeq -\frac{\alpha}{2r^4}\delta(\mathbf{r}-\mathbf{r}') \ , \tag{4}$$

where α is the target dipole polarisability. This relation illustrates the simplest correlation effect, when a charged particle induces a dipole moment on the target, which then acts back on the projectile, hence the name polarisation potential given to $-\alpha/2r^4$.

The perturbation series for Σ_ε is shown most conveniently by means of diagrams which represent the matrix element $\langle f|\Sigma_\varepsilon|i\rangle$ between some single-particle positron states i and f, figure 1. The diagrams allow one to visualise and classify the processes which contribute to the positron-atom interaction. On the other hand, each diagram corresponds to a well defined analytical expression. This opens the door for the use of one's physical intuition, without compromising the fully quantum-mechanical description of the problem.

In figure 1, the upper line with indices i and f at the ends corresponds to the positron, the wavy lines are the Coulomb interactions between the positron and atomic electrons or

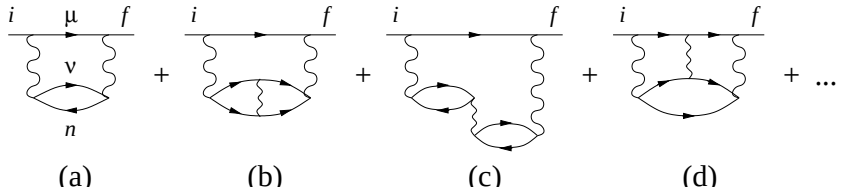

Figure 1. Many-body perturbation expansion of the correlation potential Σ_ε.

between the electrons. The other lines refer to the atom: those with arrows to the right are excited electronic states (i.e. states lying above the Fermi level), and those with arrows to the left are hole states corresponding to the orbitals occupied in the atomic ground state (at or below the Fermi level). Summation over all intermediate states is implied. For example, in diagram (a), μ is the intermediate positron state, ν is the excited electron state and n is the hole state,[b] and the corresponding analytical expression is

$$\langle f|\Sigma_\varepsilon|i\rangle = \sum_{\mu,\nu,n} \frac{\langle fn|V|\nu\mu\rangle\langle\mu\nu|V|ni\rangle}{\varepsilon - \varepsilon_\mu - \varepsilon_\nu + \varepsilon_n + i0}, \tag{5}$$

where ε_μ, ε_ν, and ε_n are the single-particle energies, and V is the Coulomb interaction. Simple diagrammatic rules allow one to write a similar expression for any of the diagrams. Of course, it is impossible to include all of them in any calculation. However, one can identify the most important diagrams or classes of diagrams, which can be summed to all orders, and thus obtain an accurate approximation for Σ_ε. This is the main idea behind all many-body theory calculations.

Note that the perturbation theory expansion in figure 1 starts with the 2nd-order diagram. The first-order diagram which describes the positron interaction with the ground-state electron density (figure 2) and similar elements within the higher-order diagrams are already included within the HF single-particle states. The diagrams are easy to interpret.

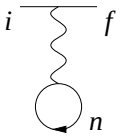

Figure 2. Positron interaction with the electron density, given analytically as $\sum_n \langle fn|V|ni\rangle$.

Thus, diagram (a) in figure 1 describes an excitation of the atom by the positron followed by the return of the electron back into its orbital. This diagram gives rise to the long-range polarisation potential (4), which is probably the most important correlation effect in low-energy scattering. However, its asymptotic behaviour corresponds to the HF polarisability, $\alpha^{\rm HF} = \frac{2}{3}\sum_{n,\nu} |\langle\nu|\mathbf{r}|n\rangle|^2/(\varepsilon_\nu - \varepsilon_n)$. To obtain a better approximation one can include higher-order corrections of the types (b) and (c) in figure 1. They describe the electron-hole

[b] All these are eigenstates of the HF Hamiltonian H_0, with the exchange interaction omitted for the positron. In the electron-atom problem the diagrammatic expansion for $\langle f|\Sigma_\varepsilon|i\rangle$ contains more diagrams, because the extra electron may exchange with the atomic electrons. As a result, there are, for example, four 2nd-order diagrams.

interaction and screening of the Coulomb interaction inside the atom, and give a substantial improvement on the simple 2nd-order diagram.[c] Let us denote this approximation $\Sigma_\varepsilon^{(\mathrm{pol})}$, since it accounts for the polarisation of the target by the charged projectile.

The many-body polarisation potential $\Sigma_\varepsilon^{(\mathrm{pol})}$ yields good results in problems involving electrons (when the exchange diagrams are also included), such as electron-atom scattering,[4,5,6] negative ions,[7,8,9] or spectra and transition amplitudes in heavy atoms with a single valence electron.[10,11] For example, figure 3(a) shows that this approach reproduces the accurate variational phaseshifts for electron-hydrogen triplet scattering.

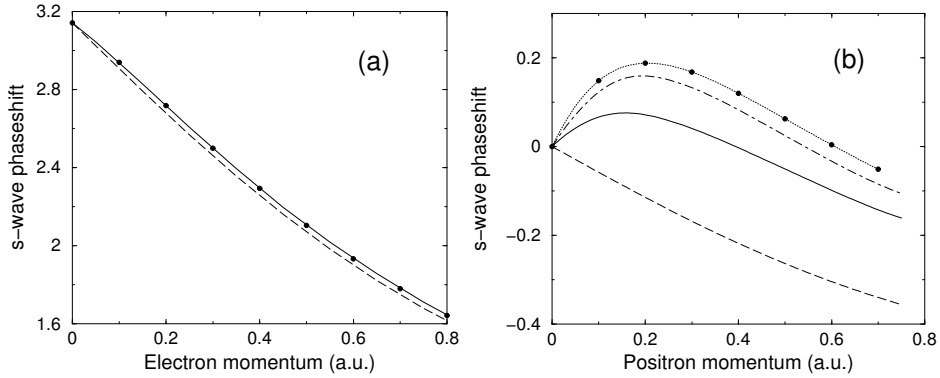

Figure 3. s-wave phaseshifts for triplet electron (a) and positron (b) scattering from hydrogen. Broken curve is the static approximation, solid curve is the many-body theory calculation with $\Sigma_\varepsilon^{(\mathrm{pol})}$, chain curve is the positron calculation with $\Sigma_\varepsilon^{(\mathrm{pol})} + \Sigma_\varepsilon^{(\mathrm{Ps})}$, and solid circles (connected by a dotted curve) are the accurate variational results for the electron [12] and positron.[13]

Scattering from the hydrogen atom is not exactly the type of problem which requires the use of many-body theory. However, it can be used to highlight the differences between electron and positron interactions with atoms. Figure 3(b) shows that in the static ("Hartree-Fock") approximation the s-wave positron-hydrogen phaseshift is negative. This is a consequence of the repulsive nature of the static positron-atom interaction which is dominated by the positron repulsion from the nucleus. The inclusion of the attractive polarisation potential $\Sigma_\varepsilon^{(\mathrm{pol})}$ changes the sign of the phaseshift at small positron energies. Therefore, effects of correlations can overcome the static positron-atom repulsion. However, as seen in figure 3(b), this approximation (which worked well for the electron) strongly underestimates the positron phaseshift. It means that in the positron-atom problem there is some additional attraction not accounted for by $\Sigma_\varepsilon^{(\mathrm{pol})}$.

One of the simplest diagrams not included in $\Sigma_\varepsilon^{(\mathrm{pol})}$ is figure 1(d). In the electron-atom problem this and similar higher-order diagrams, where the two particles in the intermediate state are connected by two, three and more Coulomb lines, form a sign-alternating series. The net result is only a small correction to $\Sigma_\varepsilon^{(\mathrm{pol})}$, which can often be neglected.[d] In the

[c] In fact, a large subset of these corrections can be incorporated within the 2nd-order diagram (a), figure 1, by simply calculating the excited electron wavefunction ν in the field of the hole n.[2]

[d] Unless someone is concerned with near-threshold double-electron ionisation (Wannier problem), where the interaction of the two slow electrons must be included to all orders.

case of positrons all contributions of this type, figure 4, have the same sign, and the total is not small. Physically, such diagrams account for the possibility of the positron forming a bound state (positronium, Ps) with one of the target electrons.

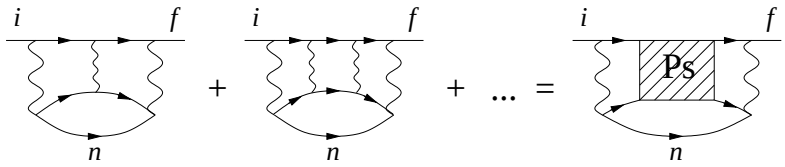

Figure 4. Ladder-diagram contributions to Σ_ε which represent virtual Ps formation.

Ps is a light analogue of the hydrogen atom, whose radius is two times greater, and energy two times smaller (i.e., $E_{1s} \approx -6.8$ eV) than the corresponding values for hydrogen. For atoms with $I > |E_{1s}|$, at positron energies below the Ps formation threshold, $\varepsilon < \varepsilon_{\rm thr} \equiv I - |E_{1s}|$, Ps can only be formed virtually. Nevertheless, this effect gives a sizeable contribution to the positron-atom attraction.[14,15] Qualitatively, this additional short-range attraction is analogous to covalent molecular bonding, with the electron moving between the parent atom and the positron.

In close-coupling calculations the effect of Ps formation is included explicitly by adding several Ps states to the expansion of the wavefunction (see, e.g., [16,17,18,19]). This method works well for hydrogen and alkali metal atoms with only one active valence electron. From a many-body theory point of view, Ps formation is taken into account by summing an infinite series of ladder-type diagrams,[e] i.e., by calculating the vertex function, figure 5.

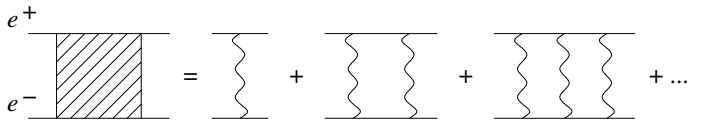

Figure 5. Electron-positron vertex function. The upper line describes the positron (e^+), and the lower line corresponds to the electron (e^-).

The vertex function (usually denoted Γ) is the central part of the *Ps-formation contribution* to the self-energy, $\Sigma_\varepsilon^{(\rm Ps)}$, figure 4. It can be found from a linear equation $\Gamma = V + VG\Gamma$, where G is the Green's function of the noninteracting electron-positron pair. This is not a trivial problem, as one has to find a way of dealing with singular Coulomb integrals between continuous spectrum states, as well as a slow convergence with respect to the orbital angular momenta of the states included.[20] In Ref. [21] we suggested an approximation for $\Sigma_\varepsilon^{(\rm Ps)}$,

$$\langle f|\Sigma_\varepsilon^{(\rm Ps)}|i\rangle = \sum_n \int \frac{\langle fn|V|\tilde{\Psi}_{1s,\mathbf{K}}\rangle\langle\tilde{\Psi}_{1s,\mathbf{K}}|V|ni\rangle}{\varepsilon + \varepsilon_n - E_{1s} - K^2/4 + i\delta} \frac{d^3K}{(2\pi)^3}, \qquad (6)$$

where $\Psi_{1s,\mathbf{K}} = \varphi_{1s}(\mathbf{r} - \mathbf{r}_1)e^{i\mathbf{K}\cdot\mathbf{R}}$ is the wave function of the ground-state Ps atom with momentum $\mathbf{K}$ and energy $E_{1s} + K^2/4$, $\mathbf{R} = (\mathbf{r} + \mathbf{r}_1)/2$ is the Ps centre of mass, and n is the

[e] It is not possible to include only a finite number of terms, because the formation of a (Ps) bound state is a nonperturbative problem.

hole, figure 4.[f] The tilde above $\Psi_{1s,\mathbf{K}}$ indicates that this wave function is orthogonalised to the occupied electron orbitals, $|\tilde{\Psi}_{1s,\mathbf{K}}\rangle = (1 - \sum_n |n\rangle\langle n|)\,|\Psi_{1s,\mathbf{K}}\rangle$. Equation (6) describes the propagation of (virtual) Ps shown by the shaded block in figure 4. At $\varepsilon > -\varepsilon_n + E_{1s}$, the integral in Eq. (6) acquires an imaginary part, and the self-energy $\Sigma_\varepsilon = \Sigma_\varepsilon^{(\mathrm{pol})} + \Sigma_\varepsilon^{(\mathrm{Ps})}$ becomes complex. This signifies the opening of the Ps formation channel.

The inclusion of the virtual Ps contribution in Σ_ε increases the positron-hydrogen s-wave phaseshift, and makes it close to the best variational results,[13] figure 3 (the agreement being even better for the p and d waves [21]).

2 Positron-atom scattering and bound states

Virtual Ps formation has an even more pronounced effect on positron interaction with heavier noble-gas atoms.[22] As an example, figure 6 shows the differential cross sections (DCS) for argon at three energies below the Ps formation threshold. It is somewhat surprising

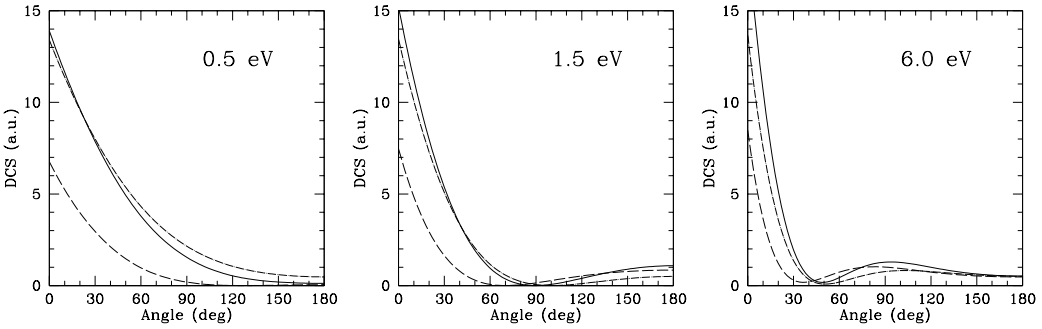

Figure 6. Differential cross sections for positron scattering from Ar. Broken curve is the many-body calculation with $\Sigma_\varepsilon^{(\mathrm{pol})}$, solid curve is that with $\Sigma_\varepsilon^{(\mathrm{pol})} + \Sigma_\varepsilon^{(\mathrm{Ps})}$ (Ref. [23]). Chain curve is the PO calculation.[24]

that our $\Sigma_\varepsilon^{(\mathrm{pol})} + \Sigma_\varepsilon^{(\mathrm{Ps})}$ calculation gives results similar to those of an earlier polarised-orbital (PO) calculation,[24] where the effect of Ps formation was completely neglected. This PO approximation calculates the positron-atom polarisation interaction for a stationary positron (i.e., assuming that it is infinitely heavy). In terms of many-body theory, this corresponds to a neglect of positron energy in the denominators of the diagrams [e.g., ε and ε_μ in Eq. (5)], and to *overestimation* of their magnitude at low positron energies.[22] As a result, at $\varepsilon \sim 1$ eV DCS from both theories are in good agreement with experiment.[25]

Figure 7 shows that at larger positron energies the result of a many-body theory calculation which accounts for both polarisation and Ps formation, is completely different from a PO calculation. The opening of the Ps formation channel at $\varepsilon_{\mathrm{thr}} \approx 9$ eV is manifested by a large onset in the total cross section σ_{tot} shown by both theory and experiment. As we saw in figure 6, the DCS are strongly forward peaked. This causes a problem with experimental determination of σ_{tot} due to a loss of forward elastically scattered particles at $\theta < \theta_R$.[30] We

[f] Ps formation in the 1s state dominates for atoms with larger ionisation potentials and smaller radii,[19,21] which justifies the neglect of excited Ps states by approximation (6).

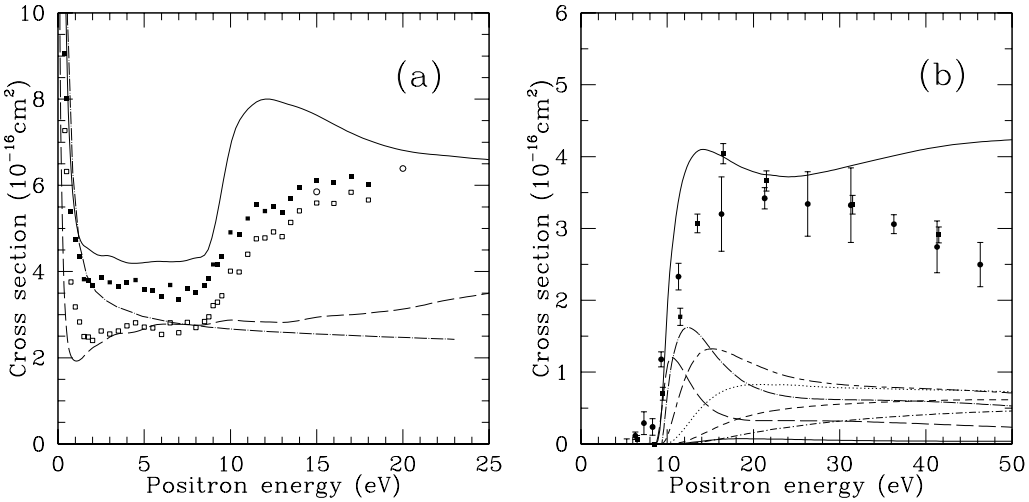

Figure 7. Positron scattering from argon. (a) shows the total scattering cross section: broken curve is obtained with $\Sigma_\varepsilon^{(\mathrm{pol})}$, solid curve is that with $\Sigma_\varepsilon^{(\mathrm{pol})}+\Sigma_\varepsilon^{(\mathrm{Ps})}$ (Ref. [23]), and chain curve is the PO calculation.[24] Experiment: open squares Ref. [26]; solid squares, the same corrected for forward-angle scattering; open circles, Ref. [27]. (b) shows the total inelastic scattering cross section obtained with $\Sigma_\varepsilon^{(\mathrm{pol})}+\Sigma_\varepsilon^{(\mathrm{Ps})}$ (thick solid curve), and its break-up into different positron partial waves (thin solid curve, s; broken curve, p; chain curve, d, etc.). Solid circles are the Ps-formation cross section of Ref. [28], and solid squares that of Ref. [29].

correct this by using the theoretical elastic scattering contribution,[19]

$$\sigma_{\mathrm{tot}}^{(\mathrm{ex-corr})} = \sigma_{\mathrm{tot}}^{(\mathrm{ex})} + 2\pi \int_0^{\theta_R} \sigma_{\mathrm{el}}^{(\mathrm{th})} \sin\theta d\theta. \tag{7}$$

The size of the onset in σ_{tot} roughly matches that of the the Ps-formation cross section σ_{Ps},[g] which is in good agreement with experiment, figure 7 (b).

Thus, we see that a many-body theory which uses $\Sigma_\varepsilon^{(\mathrm{pol})}+\Sigma_\varepsilon^{(\mathrm{Ps})}$ is capable of describing positron-atom interaction both at low energy and throughout the Ps formation threshold region. It predicts even more dramatic effects in positron-Mg scattering.[31] Magnesium has a much larger dipole polarisability and a lower ionisation threshold, and its σ_{Ps} is an order of magnitude greater than that in Ar.[32]

In the noble-gas atom sequence, the positron scattering cross sections increase substantially from He and Ne to Xe, which correlates with the increase of the atomic dipole polarisability. At low energies this is shown by the s-wave scattering lengths a, table 1. A large negative a corresponds to a positron-atom virtual level at $\varepsilon = \kappa^2/2$, where $\kappa = 1/a$.[34] Looking at Kr and Xe makes it obvious that any further increase in the strength of positron-atom attraction will cause the virtual level to become a bound state. This happens when κ crosses zero and becomes positive, giving a bound state at $\varepsilon_0 = -\kappa^2/2$.

In Ref. [35] we used this understanding to predict positron binding to four closed-shell atoms with $I > 6.8$ eV, see table 2. With the exception of mercury, the size of the binding

[g] Our theory provides the total inelastic cross section σ_{in}. It is equal to σ_{Ps} between the Ps-formation and next inelastic threshold. However, Ps formation dominates σ_{in} in a wider energy range above threshold. At higher energies σ_{in} is dominated by the positron ionisation cross section, but its onset is rather gradual.

Table 1. Positron scattering lengths for noble-gas atoms.

Quantity	He	Ne	Ar	Kr	Xe
a (a.u., Ref. [22])	–	−0.43	−3.9	−9.1	−100
a (a.u., PO [24])	−0.53	−0.55	−5.30	−10.4	−45.3
α (a.u., Ref. [33])	1.38	2.68	11.08	16.74	27.06

energy was considered as a safeguard against the uncertainty associated with the approximate treatment of $\Sigma_\varepsilon^{(\mathrm{Ps})}$. We also made a survey of the periodic table to estimate the strength of positron-atom attraction in terms of α and I, and found that many atoms are very likely to bind positrons. Following [35] and the first proof of positron-atom binding in a variational calculation for Li,[36] a large number of sophisticated calculations of positron-atom bound states have been performed. Some results obtained using a fixed-core stochastic variational method (FCSVM), and combinations of configuration interaction (CI) with model core polarisation potentials (CP) or many-body (MB) approaches, are shown in table 2. At present there are about ten atoms and a number of simple molecules where theory predicts positron binding.[37]

Table 2. Positron binding to atoms with $I > 6.8$ eV.

	Binding energies (eV)						
Method	Be	Mg	Cu	Zn	Ag	Cd	Hg
Ref. [35]	–	0.87	–	0.23	–	0.35	0.05
FCSVM [38]	0.086	0.425	0.152	0.039	0.159	–	–
CI+CP [39]	0.084	–	0.122	0.102	–	0.166	–
CI+MB [40]	–	–	0.170	–	0.123	–	–
α (a.u., Ref. [33])	38	72	40	50	67	60	34

3 Positron annihilation on atoms

Positron annihilation with electrons, with its characteristic signature of two or three γ quanta carrying away $2mc^2$ of energy, makes this particle a unique probe. Positrons send us signals from the outer space where they occur naturally. They are routinely used in the laboratory to study condensed phase systems, applied in industry to control the structure of materials, and are vital for high-resolution computer tomography in medicine. Underlying all these applications is the process of positron annihilation with atomic electrons.

The annihilation of positrons in binary collisions with atoms or molecules is usually studied in a gas, where the annihilation rate is expressed in terms of the effective number of electrons (Z_{eff}), as $\lambda = \pi r_0^2 c Z_{\mathrm{eff}} n$.[41] Here n is the gas density, $r_0 = e^2/mc^2$ is the classical electron radius, and c is the speed of light. This equation defines Z_{eff} as the ratio of the positron annihilation rate in a gas of atoms to the positron annihilation rate in a gas of uncorrelated electrons with density n. Since annihilation takes place at very small ("zero", i.e. $\sim \hbar/mc \sim 10^{-2}$ a.u.) electron-positron separations, Z_{eff} is given by [41]

$$Z_{\mathrm{eff}} = \int \sum_{i=1}^{N} \delta(\mathbf{r}_i - \mathbf{r}) |\Psi_E(\mathbf{r}_1, \ldots, \mathbf{r}_N, \mathbf{r})|^2 d\mathbf{r}_1 \ldots d\mathbf{r}_N d\mathbf{r}, \tag{8}$$

where $\Psi_E(\mathbf{r}_1, \ldots, \mathbf{r}_N, \mathbf{r})$ is normalised to the positron plane wave, Eq. (3).

Although $Z_{\rm eff}$ is basically the cross section, Eq. (8) has the appearance of a transition amplitude, $\delta(\mathbf{r}_i - \mathbf{r})$ being the "annihilation operator". This allows one to develop formally a many-body diagrammatic expansion for $Z_{\rm eff}$.[15,22]

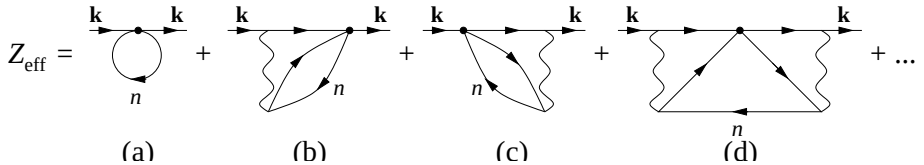

Figure 8. Diagrammatic expansion of $Z_{\rm eff}$. Solid circle is the annihilation vertex $\delta(\mathbf{r}_i - \mathbf{r})$.

Diagram (a) is the simplest uncorrelated contribution of positron annihilation on the ground-state electron density,

$$Z_{\rm eff}^{\rm (a)} = \sum_n \int |\psi_{\mathbf{k}}(\mathbf{r})|^2 |\phi_n(\mathbf{r})|^2 d\mathbf{r}, \tag{9}$$

and diagrams (b), (c), (d), etc. are the correlation corrections. Physically, they describe the enhancement of the contact electron-positron density due to their Coulomb attraction. In a binary electron-positron collision this increase is described by the so-called Gamow factor,

$$S(k) = |\psi_{\mathbf{k}}(0)|^2 / |\psi_{\mathbf{k}}(\infty)|^2 = (2\pi/k)(1 - e^{-2\pi/k})^{-1}. \tag{10}$$

Numerical calculations for noble gas atoms show [22] that the perturbation series for $Z_{\rm eff}$ converges slowly.[42] In the simplest static (HF) approximation, $Z_{\rm eff}^{\rm (a)}$ is one to two orders of magnitude smaller than the experimental values, figure 9. Even when the positron wavefunction is found from Eq. (2) with $\Sigma_\varepsilon^{\rm (pol)} + \Sigma_\varepsilon^{\rm (Ps)}$, diagram (a) alone accounts for 25% of $Z_{\rm eff}$ only. Besides a direct numerical calculation, we found an approximate way to include vertex corrections, based on the Gamow factor (10),

$$Z_{\rm eff} \approx Z_{\rm eff}^{\rm (a)} \int |\tilde{\phi}_n(\mathbf{k})|^2 S_R(k) d^3k/(2\pi)^3, \tag{11}$$

where the modified Gamow factor $S_R(k) = 2\pi(k^2 + 2/R)^{-1/2}$ is averaged over the density of the valence electron wavefunction in momentum space $\tilde{\phi}_n(\mathbf{k})$, and $R = e^2/I$ is the atomic radius. This factor gives the largest enhancement in atoms with lower I and low characteristic electron momenta (H, Xe), and the smallest effect in the opposite case (Ne). It also provides good agreement with experimental $Z_{\rm eff}$, figure 9. Note that the positron annihilation rate at low energy correlates with the magnitude of the scattering length (for hydrogen $a = -2.1$ a.u. [13]). This enhancement is proportional to $|a|^2$, and is due to the existence of a virtual (or weakly-bound) positron s level. It was first predicted in Ref. [45], rediscovered in Ref. [15] and analysed in detail in Ref. [46]. In particular, Ref. [46] shows that for room temperature positrons this mechanism can give $Z_{\rm eff}$ up to 10^3.

4 Positron annihilation on molecules

It has been known for about 40 years [47,48,49] that many molecules have large $Z_{\rm eff}$ at room temperatures, e.g., $Z_{\rm eff} = 3\,500$ for C_3H_8 (propane), and $Z_{\rm eff} = 9\,530$ for CCl_4. When

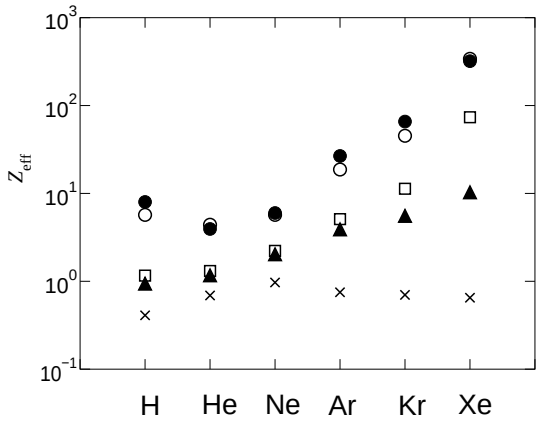

Figure 9. $Z_{\rm eff}$ for hydrogen and noble-gas atoms. Calculation (Ref. [22]): crosses, static HF values; triangles, HF+$\Sigma^{\rm (pol)}$; open squares, HF+$\Sigma^{\rm (pol)}$ + $\Sigma^{\rm (Ps)}$ [all using Eq. (9)]; open circles, same as squares, including vertex corrections, Eq. (11) (phenomenological "Gamow factor"). Solid circles show an accurate calculated value for hydrogen at $k = 0.05$,[43] and experimental room temperature values for the noble-gas atoms.[44]

studied systematically for alkanes, the experiment revealed [50] that $Z_{\rm eff}$ increases much faster than the number of electrons or atoms in the molecule, reaching 10^6 for decane. Experiments also showed a strong chemical sensitivity of $Z_{\rm eff}$. Possible mechanisms involving resonances, positron bound states, threshold effects, etc., were discussed.[49,51] Nevertheless, the situation largely remained a puzzle.

The discovery of positron binding to neutral atoms has reinforced the idea that many molecules should be capable of forming bound states with the positron. Positron capture into such bound states by emission of a photon is an unlikely process. On the other hand, the incident positron energy can be transferred into vibrations. Since vibrational motion is quantised, this will only take place at specific positron energies, corresponding to the vibrationally excited states of the positron-molecule complex. They will manifest themselves in the positron continuum as vibrational Feshbach resonances (VFR).

A true theory of positron annihilation on molecules is only emerging now.[46,52] It distinguishes two annihilation mechanisms, direct and resonant. The former operates for atoms and molecules not capable of binding positrons, and gives $Z_{\rm eff} < 10^3$. The latter involves positron capture in VFR. Within this mechanism the energy-averaged resonant contribution to $Z_{\rm eff}$ is proportional to the resonance level density, which would explain the rapid increase of $Z_{\rm eff}$ with molecular size and chemical sensitivity. Finally, the role of vibrations in high molecular $Z_{\rm eff}$ has been demonstrated directly in a state-of-the-art experiment with a trap-based low-energy monoenergetic ($\Delta\varepsilon \sim 20$ meV) positron beam.[53]

Acknowledgments

I would like to thank V. V. Flambaum who drew my attention to the positron-atom problem and, together with V. A. Dzuba and W. A. King, participated in much of the work reported above. I also thank many experimentalists and theorists in the field for useful and stimulating communications, in particular, C. M. Surko and the San Diego group whose work has advanced the positron-molecule annihilation problem enormously, W. E. Kaup-

pila, T. S. Stein and E. Surdutovich (Detroit), members of the UCL group J. Humberston, G. Laricchia and P. Van Reeth, and M. Charlton (University of Wales Swansea).

References

1. A. B. Migdal, *Theory of Finite Fermi-Systems, and Applications to Atomic Nuclei* (New York: Interscience Pub. 1967).
2. M. Ya. Amusia and N. A. Cherepkov, Case Studies in Atomic Physics **5**, 47 (1975).
3. J. S. Bell and E. J. Squires, Phys. Rev. Lett. **3**, 96 (1959).
4. H. P. Kelly, Phys. Rev. **131**, 684 (1963).
5. M. Ya. Amusia *et al.*, Phys. Rev. A **25**, 219 (1982).
6. W. R. Johnson and C. Guet, Phys. Rev. A **49**, 1041 (1994); **64**, 019901 (2001).
7. L. V. Chernysheva, G. F. Gribakin, V. K. Ivanov, M. Yu. Kuchiev, J. Phys. B **21**, L419 (1988); G. F. Gribakin, B. V. Gultsev, V. K. Ivanov, and M. Yu. Kuchiev, J. Phys. B **23** 4505 (1990).
8. V. A. Dzuba, V. V. Flambaum, G. F. Gribakin, and O. P. Sushkov, Phys. Rev. A **44**, 2823 (1991).
9. V. A. Dzuba and G. F. Gribakin, Phys. Rev. A **49**, 2483 (1994); **50** 3551 (1994).
10. V. A. Dzuba, V. V. Flambaum, P. G. Silvestrov, and O. P. Sushkov, J. Phys. B **20**, 1399 (1987); Phys. Lett. A **131**, 461 (1988); V. A. Dzuba, V. V. Flambaum, and O. P. Sushkov, *Phys. Lett. A* **140**, 493 (1989).
11. S. A. Blundell, W. R. Johnson, and J. Sapirstein Phys. Rev. A **38**, 4961 (1988).
12. C. Schwartz, Phys. Rev. **124**, 1468 (1961).
13. A. K. Bhatia, A. Temkin, R. J. Drachman, and H. Eiserike, Phys. Rev. A **3**, 1328 (1971).
14. M. Ya. Amusia, N. A. Cherepkov, L. V. Chernysheva, and S. G. Shapiro, J. Phys. B **9**, L531 (1976).
15. V. A. Dzuba *et al.*, Phys. Scripta T **46**, 248 (1993).
16. S. Guha and A. S. Ghosh, Phys. Rev. A **23**, 743 (1981).
17. R. N. Hewitt, C. J. Noble, and B. H. Bransden, J. Phys. B **25**, 2683 (1992).
18. J. Mitroy, J. Phys. B **26** 4861 (1993); J. Mitroy, L. Berge, and A. Stelbovics, Phys. Rev. Lett. **73**, 1966 (1994).
19. M. T. McAlinden, A. A. Kernoghan, and H. R. J. Walters, Hyperfine Interactions **89**, 161 (1994); J. Phys. B **28**, 1079 (1995); **29** 555 (1996); **29** 3971 (1996); **30** 1543 (1997).
20. J. Ludlow and G. F. Gribakin (work in progress).
21. G. F. Gribakin and W. A. King, J. Phys. B **27**, 2639 (1994).
22. V. A. Dzuba, V. V. Flambaum, G. F. Gribakin, and W. A. King, J. Phys. B **29**, 3151 (1996).
23. G. F. Gribakin (unpublished).
24. R. P. McEachran, D. L. Morgan, A. G. Ryman, and A. D. Stauffer, J. Phys. B **10**, 663 (1977); **11**, 951 (1978); R. P. McEachran, A. G. Ryman, and A. D. Stauffer, J. Phys. B **11**, 551 (1978); **12**, 1031 (1979); R. P. McEachran, A. D. Stauffer, and L. E. M. Campbell, *ibid* **13**, 1281 (1980).
25. S. J. Gilbert, R. G. Greaves, and C. M. Surko, Phys. Rev. Lett. **82**, 5032 (1999).
26. W. E. Kauppila, T. S. Stein, and G. Jesion, Phys. Rev. Lett. **36**, 580 (1976).
27. W. E. Kauppila *et al.*, Phys. Rev. A **24**, 725 (1981).

28. L. S. Fornari, L. M. Diana, and P. G. Coleman, Phys. Rev. Lett. **51**, 2276 (1983).
29. S. Zhou *et al.*, Phys. Rev. Lett. **73**, 236 (1994).
30. C. K. Kwan *et al.*, Phys. Rev. A **44**, 1620 (1991); S. P. Parikh *et al.*, Phys. Rev. A **47**, 1535 (1993).
31. G. F. Gribakin and W. A. King, Can. J. Phys. **74**, 449 (1996).
32. T. S. Stein *et al.*, Nucl. Instr. Meth. B **143**, 68 (1998).
33. A. A. Radtsig and B. M. Smirnov, *Parameters of Atoms and Atomic Ions: Handbook* (Energoatomizdat, Moscow, 1986).
34. L. D. Landau and E. M. Lifshitz, *Quantum Mechanics*, 3rd ed. (Pergamon, Oxford, 1977).
35. V. A. Dzuba, V. V. Flambaum, G. F. Gribakin, and W. A. King, Phys. Rev. A **52**, 4541 (1995).
36. G. G. Ryzhikh and J. Mitroy, Phys. Rev. Lett. **79**, 4124 (1997).
37. *New Directions in Antimatter Chemistry and Physics*, Eds. C. M. Surko and F. A. Gianturco (Kluwer Academic, Dordrecht, 2001).
38. G. G. Ryzhikh, J. Mitroy, and K. Varga, J. Phys. B **31**, 3965 (1998) and Refs. therein; J. Mitroy and G. G. Ryzhikh, *ibid* **34**, 2001 (2001). Also, J. Mitroy, M. W. J. Bromley, and G. G. Ryzhikh, Ch. 12 in Ref. [37].
39. J. Mitroy and G. Ryzhikh, J. Phys. B **32**, 2831 (1999); M. W. J. Bromley, J. Mitroy, and G. G. Ryzhikh, Nucl. Instr. Methods B **171** 47 (2000); M. W. J. Bromley and J. Mitroy, Phys.Rev. A **65** 012509 (2002); J. Mitroy (private communication).
40. V. A. Dzuba, V. V. Flambaum, G. F. Gribakin, and C. Harabati, Phys. Rev. A **60**, 3641 (1999); V. A. Dzuba, V. V. Flambaum, and C.Harabati, Phys. Rev. A **62**, 042504 (2000).
41. P. A. Fraser, Adv. At. Mol. Phys. **4**, 63 (1968).
42. G. F. Gribakin and J. Ludlow, J. Phys. B **35**, 339 (2002).
43. J. W. Humberston and J. B. Wallace, J. Phys. B **5**, 1138 (1972); A. K. Bhatia, R. J. Drachman, and A. Temkin, Phys. Rev. A **9**, 223 (1974); P. Van Reeth and J. W. Humberston, J. Phys. B **31**, L231 (1998).
44. P. G. Coleman, T. C. Griffith, G. R. Heyland, and T. L. Killeen, J. Phys. B. **8** 1734 (1975); G. L. Wright, M. Charlton, T. C. Griffith, and G. R. Heyland, J. Phys. B **18**, 4327 (1985).
45. V. I. Goldanskii and Yu. S. Sayasov, Phys. Lett. **13**, 300 (1964).
46. G. F. Gribakin, Phys. Rev. A **61**, 022720 (2000).
47. D. A. L. Paul and L. Saint-Pierre, Phys. Rev. Lett. **11**, 493 (1963).
48. G. R. Heyland, M. Charlton, T. C. Griffith, and G. L. Wright, Can. J. Phys. **60**, 503 (1982).
49. C. M. Surko, A. Passner, M. Leventhal, and F. J. Wysocki, Phys. Rev. Lett. **61**, 1831 (1988).
50. K. Iwata *et al.*, Phys. Rev. A **51**, 473 (1995) and references therein.
51. P. M. Smith and D. A. L. Paul, Can. J. Phys. **48**, 2984 (1970); G. K. Ivanov, Doklady Akademii Nauk SSSR **291**, 622 (1986) [Dokl. Phys. Chem. **291**, 1048 (1986)]; G. Laricchia and C. Wilkin, Phys. Rev. Lett. **79**, 2241 (1997).
52. G. F. Gribakin, Ch. 22 in Ref. [37].
53. S. J. Gilbert, L. D. Barnes, J. P. Sullivan, and C. M. Surko, Phys. Rev. Lett. **88**, 043201 (2002).